Relationship between and implications of the isotope and pressure effects on transition temperature, penetration depths and conductivities.

T. Schneider
Physik-Institut der Universität Zürich, Winterthurerstr. 190, CH-8057 Zürich, Switzerland

It is shown that the empirical relations between transition temperature, normal state conductivity linearly extrapolated to the value at the transition temperature, zero temperature penetration depths, etc., as observed in a rich variety of cuprate superconductors, are remarkably consistent with the universal critical properties of anisotropic systems which fall into the 3D-XY universality class and undergo a crossover to a quantum critical point in 2D. The variety includes n- and p-type cuprates, comprises the underdoped and overdoped regimes and the consistency extends up to six decades in the scaling variables. The resulting scaling relations for the oxygen isotope hydrostatic pressure effects agree with the experimental data and reveal that these effects originate from local lattice distortions preserving the volume of the unit cell. These observations single out 3D and anisotropic microscopic models which incorporate local lattice distortions, fall in the experimentally accessible regime into the 3D-XY universality class, and incorporate the crossover to 2D quantum criticality where superconductivity disappears.

I. INTRODUCTION

Establishing and understanding the phase diagram of cuprate superconductors in the temperature - dopant concentration plane is one of the major challenges in condensed matter physics. Superconductivity is derived from the insulating and antiferromagnetic parent compounds by partial substitution of ions or by adding or removing oxygen. For instance La_2CuO_4 can be doped either by alkaline earth ions or oxygen to exhibit superconductivity. The empirical phase diagram of $La_{2-x}Sr_xCuO_4$ [1–9] depicted in Fig. 1 shows that after passing the so called underdoped limit ($x_u \approx 0.047$), T_c reaches its maximum value T_c^m at $x_m \approx 0.16$. With further increase of x, T_c decreases and finally vanishes in the overdoped limit $x_o \approx 0.273$.

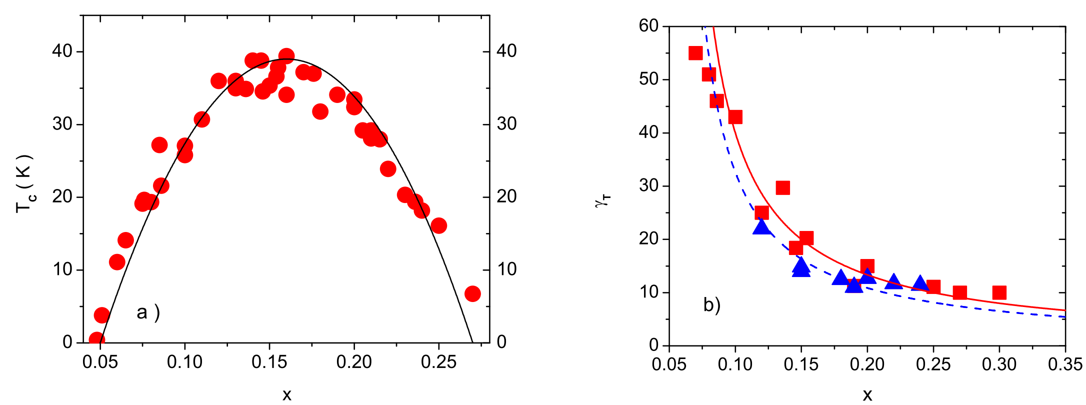

FIG. 1. a) Variation of T_c for $La_{2-x}Sr_xCuO_4$. Experimental data taken from [1–9]. The solid line is Eq.(1) with $T_c(x_m) = 39$K. b) γ_T versus x for $La_{2-x}Sr_xCuO_4$. The squares are the experimental data for γ_{T_c} [1,2,4,6,7] and the triangles for $\gamma_{T=0}$ [8,9]. The solid curve and dashed lines are Eq. (2) with $\gamma_{T_c,0} = 2$ and $\gamma_{T=0,0} = 1.63$.

This phase transition line is thought to be a generic property of cuprate superconductors [10] and is well described by the empirical relation

$$T_c(x) = T_c(x_m)\left(1 - 2\left(\frac{x}{x_m} - 1\right)^2\right) = \frac{2T_c(x_m)}{x_m^2}(x - x_u)(x_o - x), \quad x_m = 0.16, \tag{1}$$

proposed by Presland *et al.* [11]. Approaching the endpoints along the axis x, $La_{2-x}Sr_xCuO_4$ undergoes at zero temperature doping tuned quantum phase transitions. As their nature is concerned, resistivity measurements [3,12]

reveal a quantum superconductor to insulator (QSI) transition in the underdoped limit [13–16] and in the overdoped limit a quantum superconductor to normal state (QSN) transition [13–16].

Another essential experimental fact is the doping dependence of the anisotropy. In tetragonal cuprates it is defined as the ratio $\gamma = \xi_{ab}/\xi_c$ of the correlation lengths parallel (ξ_{ab}) and perpendicular (ξ_c) to CuO_2 layers (ab-planes). In the superconducting state it can also be expressed as the ratio $\gamma = \lambda_c/\lambda_{ab}$ of the London penetration depths due to supercurrents flowing perpendicular (λ_c) and parallel (λ_{ab}) to the ab-planes. Approaching a non-superconductor to superconductor transition ξ diverges, while in a superconductor to non-superconductor transition λ tends to infinity. In both cases, however, γ remains finite as long as the system exhibits anisotropic but genuine 3D behavior. There are two limiting cases: $\gamma = 1$ characterizes isotropic 3D- and $\gamma = \infty$ 2D-critical behavior. An instructive model where γ can be varied continuously is the anisotropic 2D Ising model [17]. When the coupling in the y direction goes to zero, $\gamma = \xi_x/\xi_y$ becomes infinite, the model reduces to the 1D case and T_c vanishes. In the Ginzburg-Landau description of layered superconductors the anisotropy is related to the interlayer coupling. The weaker this coupling is, the larger γ is. The limit $\gamma = \infty$ is attained when the bulk superconductor corresponds to a stack of independent slabs of thickness d_s. With respect to experimental work, a considerable amount of data is available on the chemical composition dependence of γ . At T_c it can be inferred from resistivity ($\gamma = \xi_{ab}/\xi_c = \sqrt{\rho_{ab}/\rho_c}$) and magnetic torque measurements, while in the superconducting state it follows from magnetic torque and penetration depth ($\gamma = \lambda_c/\lambda_{ab}$) data. In Fig. 1b we displayed the doping dependence of $1/\gamma_T$ evaluated at T_c (γ_{T_c}) and $T = 0$ ($\gamma_{T=0}$). As the dopant concentration is reduced, γ_{T_c} and $\gamma_{T=0}$ increase systematically, and tend to diverge in the underdoped limit. Thus the temperature range where superconductivity occurs shrinks in the underdoped regime with increasing anisotropy. This competition between anisotropy and superconductivity raises serious doubts whether 2D mechanisms and models [19], corresponding to the limit $\gamma_T = \infty$, can explain the essential observations of superconductivity in the cuprates. From Fig. 1b it is also seen that $\gamma_T(x)$ is well described by [16,18]

$$\gamma_T(x) = \frac{\gamma_{T,0}}{x - x_u}. \tag{2}$$

Having also other cuprate families in mind, it is convenient to express the dopant concentration in terms of T_c. From Eqs. (1) and(2) we obtain the correlation between T_c and γ_T:

$$\frac{T_c}{T_c(x_m)} = 1 - \left(\frac{\gamma_T(x_m)}{\gamma_T} - 1\right)^2, \quad \gamma_T(x_m) = \frac{\gamma_{T,0}}{x_m - x_u} \tag{3}$$

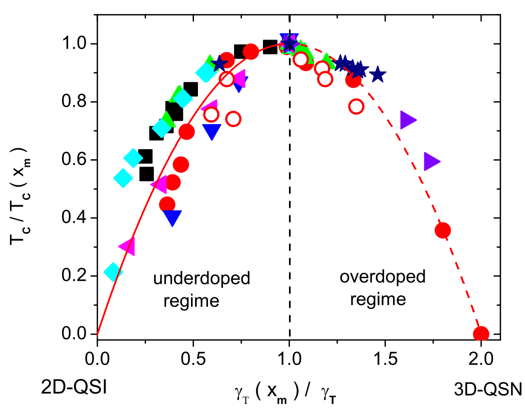

FIG. 2. $T_c/T_c(x_m)$ versus $\gamma_T(x_m)/\ \gamma_T$ for $La_{2-x}Sr_xCuO_4$ (●, $T_c(x_m) = 37$K, $\gamma_{T_c}(x_m) = 20$) [1,2,4,6,7] , (○, $T_c(x_m) = 37$K, $\gamma_{T=0}(x_m) = 14.9$) [8,9], $HgBa_2CuO_{4+\delta}$ (▲, $T_c(x_m) = 95.6$K, $\gamma_{T_c}(x_m) = 27$) [20], $Bi_2Sr_2CaCu_2O_{8+\delta}$ (★, $T_c(x_m) = 84.2$K, $\gamma_{T_c}(x_m) = 133$) [23], $YBa_2Cu_3O_{7-\delta}$ (♦, $T_c(x_m) = 92.9$K, $\gamma_{T_c}(x_m) = 8$) [24], $YBa_2(Cu_{1-y}Fe_y)_3O_{7-\delta}$ (■, $T_c(x_m) = 92.5$K, $\gamma_{T_c}(x_m) = 9$) [25], $Y_{1-y}Pr_yBa_2Cu_3O_{7-\delta}$ (▼, $T_c(x_m) = 91$K, $\gamma_{T_c}(x_m) = 9.3$) [26], $BiSr_2Ca_{1-y}Pr_yCu_2O_8$ (◄, $T_c(x_m) = 85.4$K, $\gamma_{T=0}(x_m) = 94.3$) [27] and $YBa_2(Cu_{1-y}\ Zn_y)_3O_{7-\delta}$ (►, $T_c(x_m) = 92.5$K, $\gamma_{T=0}(x_m) = 9$) [28]. The solid and dashed curves are Eq.(3), marking the flow from the maximum T_c to QSI and QSN criticality, respectively.

Provided that this empirical correlation is not merely an artefact of $La_{2-x}Sr_xCuO_4$, it gives a universal perspective on the interplay of anisotropy and superconductivity, among the families of cuprates, characterized by $T_c(x_m)$ and $\gamma_T(x_m)$. For this reason it is essential to explore its generic validity. In practice, however, there are only a few

additional compounds, including $HgBa_2CuO_{4+\delta}$ [20] and $Bi_2Sr_2CuO_{6+\delta}$, for which the dopant concentration can be varied continuously throughout the entire doping range. It is well established, however, that the substitution of magnetic and nonmagnetic impurities, depress T_c of cuprate superconductors very effectively [21,22]. To compare the doping and substitution driven variations of the anisotropy, we depicted in Fig. 2 the plot $T_c/T_c\left(x_m\right)$ versus $\gamma_T\left(x_m\right)/\gamma_T$ for a variety of cuprate families. The collapse of the data on the parabola, which is the empirical relation (3), reveals that this scaling form is well confirmed. Thus, given a family of cuprate superconductors, characterized by $T_c\left(x_m\right)$ and $\gamma_T\left(x_m\right)$, it gives a generic perspective on the interplay between anisotropy and superconductivity.

Furthermore there is the impressive empirical correlation between zero temperature penetration depths, transition temperature and normal state conductivities (extrapolated to T_c), discovered by Homes *et al.* [29]. In Fig. 3 we displayed this scaling behavior in terms of $1/\lambda_{ab}^2\left(0\right)$ *vs.* $T_c\sigma_{ab}^{dc}$ and $1/\lambda_c^2\left(0\right)$ *vs.* $T_c\sigma_c^{dc}$. Here σ_i^{dc} is the real part of the frequency dependent normal state conductivity $\sigma_i^{dc}\left(\omega\right)$ in direction i extrapolated to zero frequency.

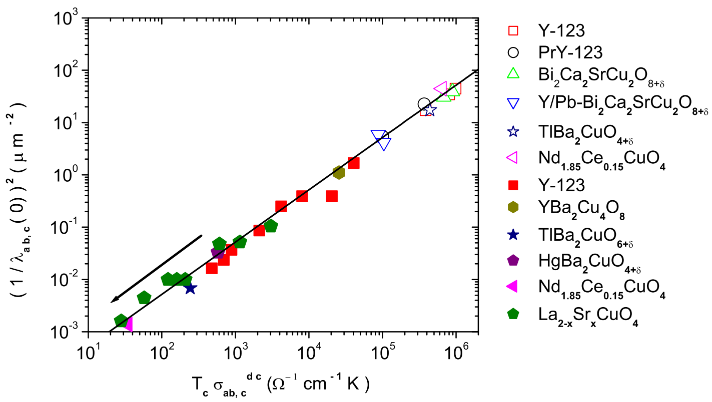

FIG. 3. $1/\lambda_{ab}^2\left(0\right)$ *vs.* $T_c\sigma_{ab}^{dc}$ (open symbols) and $1/\lambda_c^2\left(0\right)$ *vs.* $T_c\sigma_c^{dc}$ (full symbols) for various cuprates as collected by Homes *et al.* [29]. The straight line is $1/\lambda_{ab,c}^2\left(0\right) = 5.2\ 10^{-5}\ T_c\sigma_{ab,c}^{dc}$. The experimental data is taken from [30–35] for $YBa_2Cu_3O_{7-\delta}$ (Y-123), [32] for Pr-$YBa_2Cu_3O_{7-\delta}$(PrY-123), [33,36] for $YBa_2Cu_4O_8$, [33,36] for $Tl_2Ba_2CuO_{6+\delta}$, [32,37] for $Bi_2Ca_2SrCu_2O_{8+\delta}$ and Y/Pb- $Bi_2Ca_2SrCu_2O_{8+\delta}$, [38,39] for $Nd_{1.85}Ce_{0.15}CuO_4$, [29,40] for $La_{2-x}Sr_xCuO_4$(214), and [29] for $HgBa_2CuO_{4+\delta}$. The arrow indicates the flow to the 2D-QSI critical point.

Noting that the linear relationship extends over six decades it provides unprecedented evidence for universal behavior. Indeed, the data encompasses the slightly underdoped and overdoped regime of a variety of cuprates. An important implication is that the changes ΔT_c, $\Delta\left(1/\lambda_{ab,c}^2\right)$ and$\Delta\sigma_{ab,c}^{dc}$, e.g. induced by isotope exchange, are not independent but related by

$$\frac{\Delta T_c}{T_c} + 2\frac{\Delta\lambda_{ab,c}\left(0\right)}{\lambda_{ab,c}\left(0\right)} = -\frac{\Delta\sigma_{ab,c}^{dc}}{\sigma_{ab,c}^{dc}}. \tag{4}$$

Such scaling behavior differs drastically from the isotope effects in the so called conventional superconductors. In these materials mean-field treatments including the BCS theory apply and for elemental superconductors T_c scales roughly as $M^{-1/2}$, where M is the mass of the ions. Historically, the resulting isotope effect on T_c identified the phonons as the bosons mediating superconductivity. Furthermore, the isotope effect on the penetration depth, entering via the electron-phonon interaction mediated renormalization of the fermi-velocity, appears to be negligibly small.

Given the critical line $T_c\left(x\right)$ with the 2D-QSI and 3D-QSN endpoints (see Fig. 1) such universal relations are not unexpected but a consequence of fluctuations [14,16,41,42]. As an example we consider the universal scaling relation at the 2D-QSI transition [13–16,43],

$$T_c = \frac{\Phi_0^2 R_2}{16\pi^3 k_B}\frac{d_s}{\lambda_{ab}^2\left(0\right)}, \tag{5}$$

which holds independently of the nature of the putative quantum critical point. $\lambda_{ab}\left(0\right)$ is the zero temperature in-plane penetration depth, d_s the thickness of the sheets and R_2 is a universal number. Since $T_c \propto d_s/\lambda_{ab}^2\left(0\right) \propto n_s^\square$, where $n_s^\square$ is the aerial superfluid density, is a characteristic 2D property, it also applies to the onset of superfluidity in ^{4}He films adsorbed on disordered substrates, where it is well confirmed [44]. A great deal of experimental work

has also been done in cuprates on the so called Uemura plot [45], revealing an empirical correlation between T_c and $d_s/\lambda_{ab}^2(0)$.

This work aims to review the evidence that the empirical scaling relations between $\lambda_{ab,c}(0)$,T_c, d_s, $\sigma_{ab,c}^{dc}$, etc., as well as the resulting relations for the isotope and pressure effects, reflect 3D-XY universality along the phase transition line $T_c(x)$ and the crossover to the 2D-QSI quantum critical point (see Fig. 1). Although there is considerable evidence that cuprates fall into the 3D-XY universality class [14,16,46,47], the inhomogeneity induced finite size effects [46,47] and the crossovers to 2D-QSI and 3D-QSN criticality make it difficult to extract critical exponents unambiguously. For this reason we concentrate on the universal relations between critical amplitudes, their zero temperature counterparts and T_c, because these quantities can be measured with reasonable accuracy.

The paper is organized as follows. In Sec.II we sketch the universal relations for anisotropic type II superconductors falling into the 3D-XY universality class and undergo a crossover to 2D-QSI criticality. Expressing the critical amplitudes of the penetration depths in terms of their zero temperature counterparts, we find remarkable agreement with the plot shown in Fig. 3 and the experimental data for $La_{2-x}Sr_xCuO_4$ [9,45,48–50] and $Pr_{2-x}Ce_xCuO_{4-\delta}$ [51], where the doping dependence of the quantities of interest have been studied. In this context it should be recognized that the ratio between the critical amplitudes of the penetration depths and their zero temperature counterparts is not expected to be universal. However, the impressive agreement reveals that the doping and family dependence of this ratio is rather weak. In any case, the unprecedented consistency of the experimental data with 3D-XY universality and the crossover to the 2D-QSI critical point, together with the evidence for the competition between anisotropy and superconductivity raise again serious doubts whether 2D mechanisms and models [19] can explain these essential observations.

As the isotope effects are concerned, we confirm previous scaling relations between the effect on transition temperature and penetration depths [52,53] and derive new relations including the isotope effect on the conductivity and Hall constant. Furthermore, the origin of the oxygen isotope effects is traced back to a change of the c-axis correlation length. It implies a change of d_s, a shift of the underdoped limit (x_u in Fig. 1) and a reduction of the concentration of mobile carriers, accompanied by a change of the Hall constant. Noting that the change of the lattice constants upon oxygen isotope exchange is negligibly small [54,55] these isotope shifts reveal the existence and relevance of the coupling between the superfluid and volume preserving local lattice distortions. Furthermore, we review the experimental data for the combined isotope and finite size effects [56]. They open a door to probe the coupling between local lattice distortions and superconductivity rather directly in terms of the isotope shift of L_c, the spatial extent of the homogeneous superconducting grains along the c-axis. Noting that $\Delta L_c/L_c$ is rather large this change confirms the coupling between superfluidity and local lattice distortion and this coupling is likely important in understanding the pairing mechanism. Finally it is shown that the effect of hydrostatic pressure on the transition temperature and the in-plane penetration depth of $YBa_2Cu_4O_8$ [57] is consistent with 3D-XY universality as well. Thus the remarkable agreement with 3D-XY scaling and the evidence for the crossover to the 2D-QSI quantum critical point single out 3D and anisotropic microscopic models which incorporate local lattice distortions, fall in the experimentally accessible regime into the 3D-XY universality class, and incorporate the crossover to 2D-QSI criticality where superconductivity disappears.

II. EXPERIMENTAL EVIDENCE FOR THE UNIVERSAL 3D-XY- AND 2D-QSI- SCALING RELATIONS AND THEIR IMPLICATIONS

It is well-established that strongly type-II materials should exhibit a continuous normal to superconductor phase transition, and that sufficiently close to T_c, the charge of the order parameter field becomes relevant [58]. However, in cuprate superconductors within the fluctuation dominated regime, the region close to T_c where the system crosses over to the regime of charged fluctuations turns out to be too narrow to access. For instance, optimally doped $YBa_2Cu_3O_{7-\delta}$, while possessing an extended regime of critical fluctuations, is too strongly type-II to observe charged critical fluctuations [14,16]. Indeed, the effective dimensionless charge $\widetilde{e} = \xi/\lambda = 1/\kappa$ is in strongly type II superconductors ($\kappa >> 1$) small. The crossover upon approaching T_c is thus initially to the critical regime of a weakly charged superfluid where the fluctuations of the order parameter are essentially those of an uncharged superfluid or XY-model [59]. Furthermore, there is the finite size effect due to inhomogeneities which makes the asymptotic critical regime unattainable [46,47]. Thus, as long as the charge of the pairs is negligibly small the cuprates are expected to fall along the phase transition line $T_c(x)$ into the 3D-XY universality class. A universality class is not only characterized by its critical exponents but also by various critical-point amplitude combinations [41]. In particular 3D-XY universality

extended to anisotropic systems [14,16] then implies that the transition temperature T_c and the critical amplitudes of the penetration depths λ_{ab0} and transverse correlation lengths ξ_{ab0}^{tr} are not independent but related by [14,16]

$$k_B T_c = \frac{\Phi_0^2}{16\pi^3}\frac{\xi_{ab0}^{tr}}{\lambda_{ab0}^2} = \frac{\Phi_0^2}{16\pi^3}\frac{\xi_{c0}^{tr}}{\lambda_{c0}^2}, \tag{6}$$

where $\lambda_i^2(T) = \lambda_{i0}^2 t^{-\nu}$ and $\xi_i^t(T) = \xi_{i0}^t t^{-\nu}$ with $t = 1 - T/T_c$ and $\nu \simeq 2/3$. For our purpose it is convenient to replace the transverse correlation length by the corresponding correlation lengths above T_c in terms of [14,16,42]

$$\frac{\xi_{ab0}^{tr}}{\xi_{c0}} = f \approx 0.453, \ \frac{\xi_{c0}^{tr}}{\xi_{ab0}} = \gamma f, \tag{7}$$

where the anisotropy is given by

$$\gamma^2 = \left(\frac{\lambda_{c0}}{\lambda_{ab0}}\right)^2 = \frac{\xi_{c0}^{tr}}{\xi_{ab0}^{tr}} = \left(\frac{\xi_{ab0}}{\xi_{co}}\right)^2. \tag{8}$$

Combining Eqs.(6) and (7) we obtain the universal relation

$$T_c \lambda_{ab0}^2 = \frac{\Phi_0^2 f}{16\pi^3 k_B}\xi_{c0}. \tag{9}$$

It holds, as long as cuprates fall into the 3D-XY universality class, irrespective of the doping dependence of T_c, λ_{ab0}^2 and ξ_{c0}. For this reason it provides a sound basis for universal plots. However, there is the serious drawback that reliable experimental estimates for T_c and the critical amplitudes λ_{ab0} and ξ_{c0} measured on the same sample are not yet available. Nevertheless, some progress can be made by noting that by approaching the 2D-QSI transition the universal scaling form (9) should match with Eq. (5). This requires

$$\lambda_{ab0} = \Lambda_{ab}\lambda_{ab}(0), \ f\xi_{c0}/\Lambda_{ab}^2 \rightarrow R_2 d_s, \tag{10}$$

so that away from 2D-QSI criticality

$$T_c \lambda_{ab}^2(0) \simeq \frac{\Phi_0^2 f}{16\pi^3 k_B}\frac{\xi_{c0}}{\Lambda_{ab}^2}, \tag{11}$$

holds. In Fig. 4 we displayed T_c *vs.* $1/\lambda_{ab}^2(0)$ for $La_{2-x}Sr_xCuO_4$ taken from Uemura *et al.* [45,48] and Panagopoulos *et al.* [9]. The straight line is Eq. (5) with $R_2 d_s = 6.5$Å and the arrow indicates the flow to 2D-QSI transition criticality. Thus, when both T_c and $1/\lambda_{ab}^2(0)$ increase, T_c values below $T_c = \left(\Phi_0^2 R_2/6\pi^3 k_B\right) d_s/\lambda_{ab}^2(0)$ (Eq. (5)) require ξ_{c0} to fall off from its limiting value $\xi_{c0} = d_s R_2 \Lambda_{ab}^2/f$.

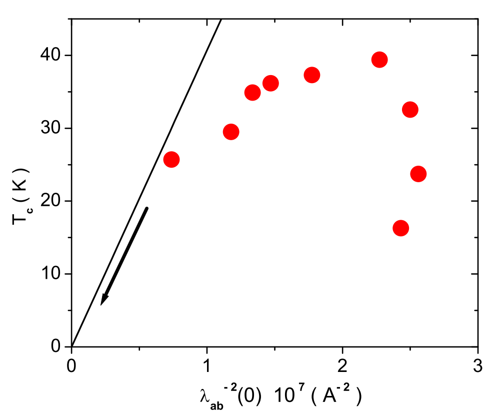

FIG. 4. T_c *vs.* $1/\lambda_{ab}^2(0)$ for $La_{2-x}Sr_xCuO_4$. Data taken from Uemura *et al.* [45,48] and Panagopoulos *et al.* [9]. The straight line is Eq. (5) with $R_2 d_s = 6.5$Å and the arrow indicates the flow to 2D-QSI transition criticality.

The doping dependence of ξ_{c0}/Λ_{ab}^2 deduced from Eq. (11) and the experimental data for T_c and $\lambda_{ab}^2(0)$ is displayed in Fig. 5a in terms of $T_c\lambda_{ab}^2(0) \propto \xi_{c0}/\Lambda_{ab}^2$ *vs.* T_c and $T_c\lambda_{ab}^2(0) \propto \xi_{c0}/\Lambda_{ab}^2$ *vs.* x . Approaching the underdoped limit ($x \approx 0.05$), where T_c vanishes (Fig. 1) and the 2D-QSI transition occurs, ξ_{c0}/Λ_{ab}^2 increases nearly linearly with decreasing x to approach a fixed value. Indeed, the data is consistent with

$$\xi_{c0}/\Lambda_{ab}^2 = \left(16\pi^3 k_B/\left(\Phi_0^2 f\right)\right) T_c\lambda_{ab}^2(0) \approx 14.34 - 60.47(x - 0.05)\text{Å}, \tag{12}$$

yielding the limiting value $\xi_{c0}(x = 0.05)/\Lambda_{ab}^2 \approx 14.34$Å and $f\xi_{c0}(x = 0.05)/\Lambda_{ab}^2 = R_2 d_s \approx 6.5$Å used in Fig. 4. An essential result is that ξ_{c0} adopts in the underdoped limit ($x \simeq 0.05$) where the 2D-QSI transition occurs and T_c vanishes its maximum value $\Lambda\xi_{c0}/\Lambda_{ab}^2 \approx 14.34$Å, which is close to the c-axis lattice constant $c \simeq 13.29$Å. Thus, a finite transition temperature requires a reduction of ξ_{c0}, well described over an unexpectedly large doping range by Eq. (12). with the doping dependence of γ (Eq. (2)) Eq. (8) transforms to

$$\xi_{c0}/\Lambda_{ab}^2 \approx 14.34 - 60.47\gamma_0/\gamma\text{Å}, \tag{13}$$

revealing that the doping dependence of the c-axis correlation length ξ_{c0} is intimately related to the anisotropy γ. Hence, a finite T_c requires unavoidably a finite anisotropy γ.

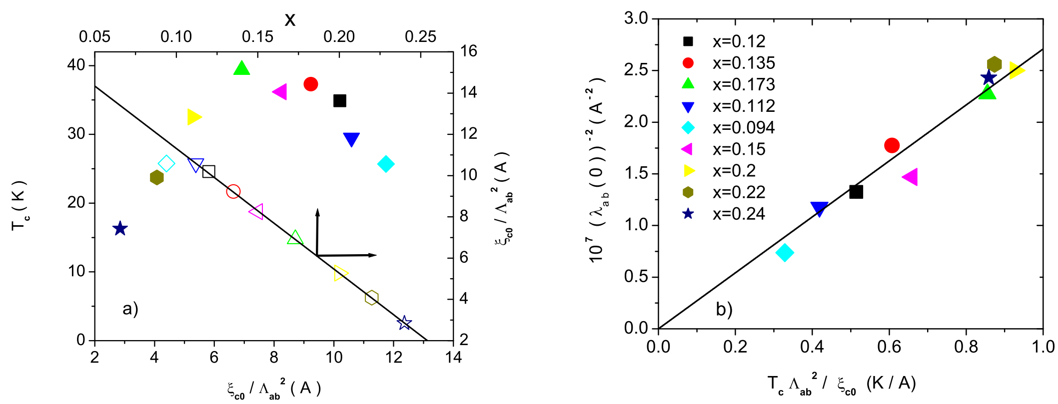

FIG. 5. a) $T_c\lambda_{ab}^2(0) \propto \xi_{c0}/\Lambda_{ab}^2$ *vs.* T_c and $T_c\lambda_{ab}^2(0) \propto \xi_{c0}/\Lambda_{ab}^2$ *vs.* x for $La_{2-x}Sr_xCuO_4$. Data taken from Pangopoulos *et al.* [9] and Uemura *et al.* [48]. The solid line indicates the behavior in the underdoped and the dashed one in the overdoped regime, while the dotted line corresponds to Eq. (12) in the form $T_c\lambda_{ab}^2(0) = 37 - 156(x - 0.047)$. b) $1/\lambda_{ab}^2(0)$ *vs.* $\Lambda_{ab}^2 T_c/\xi_{c0}$ for the same data with ξ_{c0}/Λ_{ab}^2 given by Eq. (12). The straight line is $1/\lambda_{ab}^2(0) = 2.71\ T_c\Lambda_{ab}^2/\xi_{c0}$.

The lesson is, that superconductivity in $La_{2-x}Sr_xCuO_4$ is an anisotropic but 3D phenomenon which disappears in the 2D limit. From the plot $1/\lambda_{ab}^2(0)$ *vs.* $\Lambda_{ab}^2 T_c/\xi_{c0}$ displayed in Fig. 5b, where according to Eq.(11) universal behavior is expected to occur, the data is seen to fall rather well on a straight line. This is significant, as moderately underdoped, optimally and overdoped $La_{2-x}Sr_xCuO_4$ falling according to Fig. 4 well off the 2D-QSI behavior $T_c \propto 1/\lambda_{ab}^2(0)$ now scale nearly onto a single line. Thus the approximate 3D-XY scaling relation (11), together with the empirical doping dependence of the c-axis correlation length (Eqs. (12) and (13)) are consistent with the available experimental data for $La_{2-x}Sr_xCuO_4$ and uncovers the relevance of the anisotropy. However, the linear doping dependence of ξ_c is not expected to hold closer to the overdoped limit ($x \approx 0.27$) where a 3D quantum superconductor to normal state (3D-QSN) transition is expected to occur [14,16]. Clearly, a full test of the scaling relation (11) requires independent experimental data for the critical amplitude ξ_{ab0} of the in-plane correlation length. To identify the observable probing this correlation length we note that close to 2D-QSI criticality the sheet conductivity and conductivity are related by $\sigma_{sheet} = d_s\sigma_{ab}^{dc}$ so that the universal relation (5) can be rewritten in the form

$$\frac{1}{\lambda_{ab}^2(0)\, T_c\sigma_{ab}^{dc}} = \frac{16\pi^3 k_B}{\Phi_0^2 R_2 \sigma_{sheet}}, \quad \sigma_{sheet} = \frac{h}{4e^2}\sigma_0 \simeq \sigma_0\ 1.55\ 10^{-4}\Omega^{-1}, \tag{14}$$

where $h/4e^2 = 6.45\text{k}\Omega$ is the quantum of resistance and σ_0 is a dimensionless constant of order unity [60]. Away from 2D-QSI criticality ξ_{c0} can be expressed as

$$1/\xi_{c0} \simeq \sigma_{ab}/s_{ab} = 1/\left(\rho_{ab}s_{ab}\right), \tag{15}$$

with ρ_{ab} determined from $\rho_{ab}(T)$ above T_c by linear extrapolation yielding $\rho_{ab} = \rho_{ab}(T_c^+)$. Up to the non-universal factor $s_{ab}(\Omega^{-1})$ this resistivity is expected to reflect the doping dependence of the critical amplitude ξ_{c0}. To demonstrate this behavior we displayed in Fig. 6 ρ_{ab} *vs.* x for $La_{2-x}Sr_xCuO_4$ derived from the data of Komiya *et al.* [49] and Sato *et al.* [50]. ρ_{ab} is derived from $\rho_{ab}(T)$ by linear extrapolation yielding $\rho_{ab} = \rho_{ab}(T_c^+)$. The solid line points to a nearly linear doping dependence, consistent with the behavior shown in Fig. 5a, derived from $T_c\lambda_{ab}^2(0) \propto \xi_{c0}/\Lambda_{ab}^2$ *vs.* x. Consequently, according to Eq. (11) data for T_c, $\lambda_{ab}^2(0)$ and ρ_{ab}, measured on the same sample at various dopant concentrations, should then scale as

$$\frac{1}{\lambda_{ab}^2(0)\, T_c\sigma_{ab}} = \frac{\rho_{ab}}{\lambda_{ab}^2(0)\, T_c} \simeq \frac{16\pi^3 k_B \Lambda_{ab}^2}{\Phi_0^2 f s_{ab}}. \tag{16}$$

Thus, in the plot $1/\lambda_{ab}^2(0)$ *vs.* $T_c\sigma_{ab}$ or T_c/ρ_{ab} the data should tend to fall on a straight line, while deviations are attributable to the non-universal nature of the ratio Λ_{ab}^2/s_{ab}. Indeed Λ_{ab}^2/s_{ab} does not necessarily adopt a unique value.

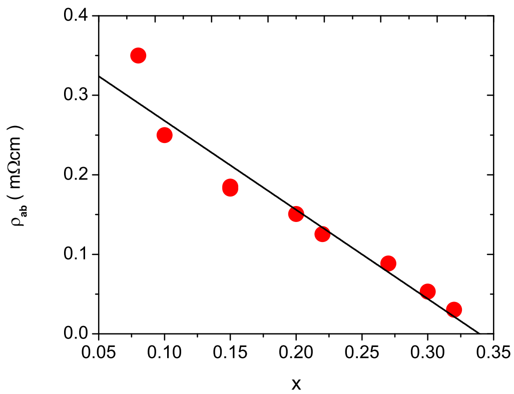

FIG. 6. ρ_{ab} *vs.* x for $La_{2-x}Sr_xCuO_4$ derived from the data of Komiya *et al.* [49] and Sato *et al.* [50]. ρ_{ab} is determined above T_c from $\rho_{ab}(T)$ in terms of a linear extrapolation yielding $\rho_{ab} = \rho_{ab}(T_c^+)$. The solid line indicates the consistency with a nearly linear doping dependence.

To demonstrate that this behavior is not an artefact of $La_{2-x}Sr_xCuO_4$ we displayed in Fig. 7a the μSR data T_c *vs.* $\sigma(0) \propto 1/\lambda_{ab}^2(0)$ for $Y_{0.8}Ca_{0.2}Ba_2(Cu_{1-y}Zn_y)O_{7-\delta}$($Y_{0.8}Ca_{0.2}$-123), $Tl_{0.5-y}Pb_{0.5+y}Sr_2Ca_{1-x}Y_xCu_2O_7$(Tl-1212) and $TlBa_2CuO_{6+\delta}$(Tl-2201) taken from Bernhard *et al.* [61] and Niedermayer *et al.* [62]. Noting that in these materials the relationship between T_c, $1/\lambda_{ab}^2(0)$ and the dopant concentration is much less obvious, we displayed in Fig. 7b the behavior of the critical amplitude of the c-axis correlation length in terms of T_c *vs.* $T_c/\sigma(0) \propto T_c\lambda_{ab}^2(0) \propto \xi_{c0}$. Noting that in analogy to $La_{2-x}Sr_xCuO_4$ (see Fig. 4) T_c *vs.* $\sigma(0) \propto 1/\lambda_{ab}^2(0)$ resembles the outline of a fly's wing, it becomes evident that the behavior of T_c *vs.* ξ_{c0}, resembling the doping dependence of T_c in $La_{2-x}Sr_xCuO_4$ (see Fig. 5a), appears to be generic. At the 2D-QSI transition ξ_{c0} adopts a finite value $\xi_{c0} = d_s R_2 \Lambda_{ab}^2/f$, it decreases with increasing transition temperature and decreases further as the maximum transition temperature is passed.

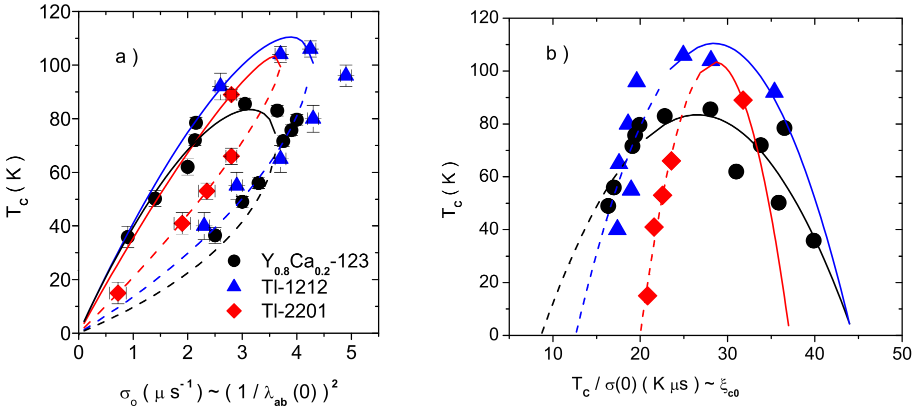

FIG. 7. a) T_c *vs.* $\sigma(0) \propto 1/\lambda_{ab}^2(0)$ for $Y_{0.8}Ca_{0.2}$-123, Tl-1212 and Tl-2201 taken from Bernhard *et al.* [61] and Niedermayer *et al.* [62]. The solid curves indicate the flow from optimum doping to 2D-QSI criticality and the dashed ones the crossover to the 3D-QSN transition in the overdoped limit. b) T_c *vs.* $T_c/\sigma(0) \propto T_c\lambda_{ab}^2(0) \propto \xi_{c0}$ for the same data. The solid lines indicate the underdoped and the dashed ones the overdoped regime.

Further evidence for this behavior stems from the in-plane penetration and resistivity data of Kim *et al.* [43]for the n-type cuprate $Pr_{2-x}Ce_xCuO_{4-\delta}$, which extends over the range $0.124 \leq x \leq 0.144$. From Fig. 8a it is seen that in analogy to p-doping there is an insulator to superconductor quantum transition at some x_u. For $x > x_u$ T_c increases monotonically, adopts its maximum value at optimum p-doping and decreases in the overdoped regime. Given this analogy between the doping dependence of T_c of p- and n-type cuprates one expects that T_c *vs.* $1/\lambda_{ab}^2(0)$ uncovers essentially the behavior of the p-type cuprates shown in Figs. 4 and 7a. A glance to Fig. 8b shows that this indeed the case. Accordingly, $Pr_{2-x}Ce_xCuO_{4-\delta}$ is expected to undergo a 2D-QSI transition at some x_u.

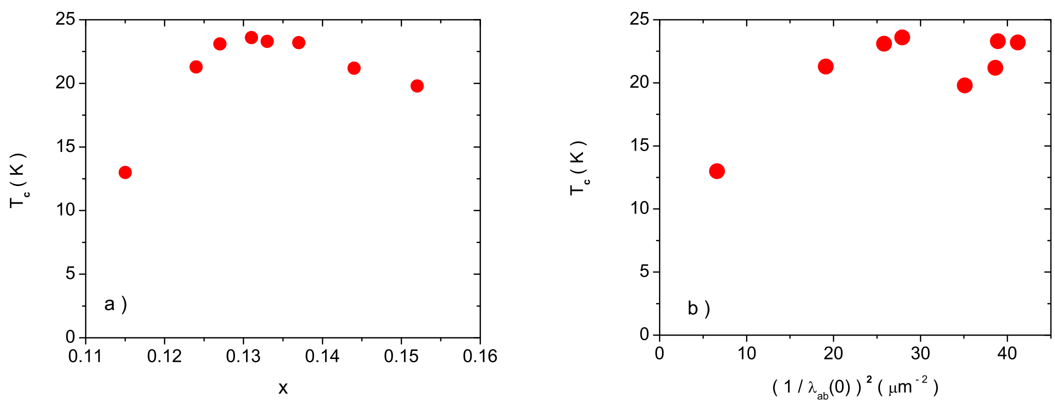

FIG. 8. a) T_c *vs.* x for $Pr_{2-x}Ce_xCuO_{4-\delta}$; b) T_c *vs.* $1/\lambda_{ab}^2(0)$. Data taken from Kim *et al.* [51].

Indeed the doping dependence of $\xi_{c0} \propto T_c\lambda_{ab}^2(0)$ displayed in Fig. 9a is rather analogous to that in $La_{2-x}Sr_xCuO_4$ shown in Fig. 5a and ξ_{c0} is seen to scale as ρ_{ab}, in agreement with Eq. (16). In this view it is not surprising that in the plot $1/\lambda_{ab}^2(0)$ *vs.* T_c/ρ_{ab} shown in Fig.9b the data fall nearly on a straight line. The solid and dashed lines will be discussed later.

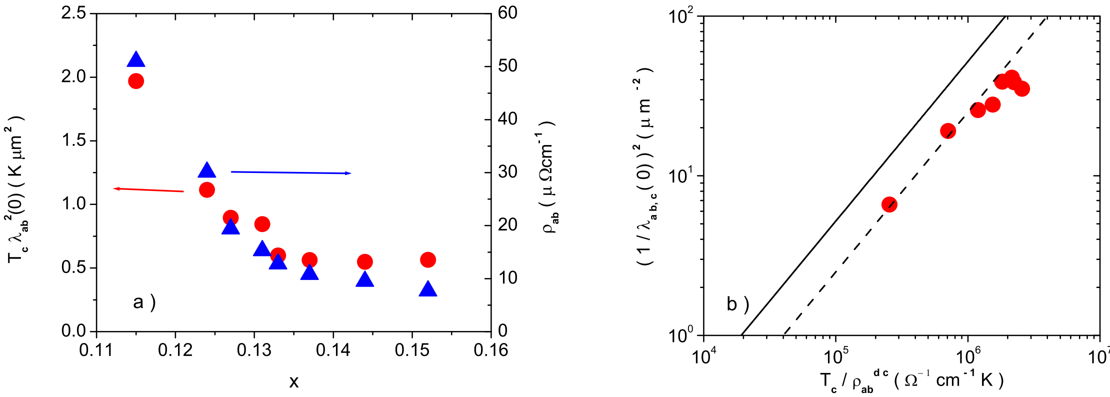

FIG. 9. a) $\xi_{c0} \propto T_c \lambda_{ab}^2(0)$ $vs.$ x and ρ_{ab} $vs.$ x for $Pr_{2-x}Ce_xCuO_{4-\delta}$ derived from the data of Kim *et al.* [43]; b) $1/\lambda_{ab}^2(0)$ $vs.$ T_c/ρ_{ab} for the same data. The solid lines line is $1/\lambda_{ab}^2(0) = 5.2\ 10^{-5}\ T_c/\rho_{ab}$ and the dashed one $1/\lambda_{ab}^2(0) = 2.5\ 10^{-5}$ T_c/ρ_{ab}.

In any case, since Eq. (9) is universal, it holds for all cuprates falling in the accessible critical regime into the 3D-XY universality class, irrespective of the doping dependence of T_c, λ_{ab0}^2, γ and ξ_{c0}. Since charged criticality is accessible in the heavily underdoped regime only [63], Eq. (9) rewritten in the form

$$\frac{\xi_{c0}}{\lambda_{ab0}^2 T_c} = \frac{\xi_{ab0}\gamma_{T_c}}{\lambda_{c0}^2 T_c} = \frac{16\pi^3 k_B}{\Phi_0^2 f}, \tag{17}$$

provides a sound basis for universal plots. However, as aforementioned there is the serious drawback that reliable experimental estimates for the critical amplitudes and the anisotropy at T_c measured on the same sample and for a variety of cuprates are not yet available. Nevertheless, as in the case of $La_{2-x}Sr_xCuO_4$ outlined above, progress can be made by invoking the approximate scaling form (11), by expressing the critical amplitude of the penetration depths by there zero temperature counterparts (Eq.(10)). The universal relation (17) transforms then to

$$\frac{\xi_{c0}}{\lambda_{ab}^2(0)\, T_c} \simeq \frac{\gamma_{T_c}\xi_{ab0}}{\lambda_c^2(0)\, T_c}\frac{\Lambda_{ab}^2}{\Lambda_c^2} \simeq \frac{16\pi^3 k_B \Lambda_{ab}^2}{\Phi_0^2 f},\ \ \frac{\Lambda_c}{\Lambda_{ab}} = \frac{\gamma_{T=0}}{\gamma_{T_c}}, \tag{18}$$

which will be used to explore the relationship between the isotope effects on the transition temperature and the zero temperature penetration depths. As aforementioned a full test of this scaling form requires an independent experimental determination of the critical amplitudes of the correlation lengths ξ_{ab0} and ξ_{c0}. We have seen that this is achieved in terms of the conductivity. Introducing σ_i^{dc}, the real part of the frequency dependent conductivity $\sigma_i^{dc}(\omega)$ in direction i extrapolated to zero frequency at $T \gtrsim T_c$ [29], one obtains in analogy to Eq. (11)

$$1/\xi_{c0} \simeq \sigma_{ab}^{dc}/s_{ab},\ 1/\left(\gamma_{T_c}\xi_{ab0}\right) \simeq \sigma_c^{dc}/s_c, \tag{19}$$

with s_i in units Ω^{-1}. With that the relation (18) transforms to

$$\frac{1}{\lambda_{ab}^2(0)\, T_c\sigma_{ab}^{dc}} \simeq \frac{1}{\lambda_c^2(0)\, T_c\sigma_c^{dc}}\frac{\Lambda_{ab}^2}{\Lambda_c^2} \simeq \frac{16\pi^3 k_B \Lambda_{ab}^2}{\Phi_0^2 f s_{ab}},\ \ \frac{\Lambda_c}{\Lambda_{ab}} = \frac{\gamma_{T_c}}{\gamma_{T=0}}, \tag{20}$$

because $\sigma_{ab}^{dc}/\sigma_c^{dc} = \gamma^2$ and with that $s_{ab} = s_c$. To check this relation we note that the 2D-QSI scaling form (14) yields

$$\frac{1}{\lambda_{ab}^2(0)\, T_c\sigma_{ab}^{dc}} \simeq \frac{10.3\ 10^{-5}}{R_2\sigma_0}, \tag{21}$$

with $\lambda_{ab}(0)$ in μm, T in K and σ_{ab}^{dc} in $(\Omega^{-1}\text{cm}^{-1})$, the structure of the ab-expression is recovered.

In Fig. 3 we displayed $1/\lambda_{ab}^2(0)$ $vs.$ $T_c\sigma_{ab}^{dc}$ and $1/\lambda_c^2(0)$ $vs.$ $T_c\sigma_c^{dc}$ as collected by Homes *et al.* [29]. Noting that the linear relationship extends over six decades this plot represents unprecedented evidence that all these cuprates fall into the 3D-XY universality class, where the approximate scaling form (18) applies. Since the ab-plane and c-axis data are well described by the same line, namely $1/\lambda_{ab,c}^2(0) \simeq 5.2\ 10^{-5} T_c\sigma_{ab,c}^{dc}$, it follows that $\Lambda_{ab}^2/\Lambda_c^2$ is close

to one and Λ_{ab}^{2}/s_{ab} adopts a nearly unique value. Note that such line is also consistent with the 2D-QSI scaling form (21). In particular for $R_2\sigma_0 \cong 1.98$ these lines coincide. The fact that all points of $1/\lambda_{ab}^{2}(0)$ *vs.* $T_c\sigma_{ab}^{dc}$ (open symbols) nearly fall onto a single line is significant, as moderately underdoped, optimally and overdoped materials, which fell well off of the 2D-QSI behavior $T_c \propto 1/\lambda_{ab}^{2}(0)$ (see Figs. 4, 7a, and 8a) now scale nearly onto a single line, in agreement with Figs. 5b and 9b. Although the agreement, extending over 6 decades in the scaling variables is impressive, the plot $\lambda_{ab,c}^{2}(0)\,T_c\sigma_{ab,c}^{dc}\ 5.210^{-4}$ *vs.* $1/\ \lambda_{ab,c}^{2}(0)$ displayed in Fig. 10 reveals that there are deviations, ascribable to experimental uncertainties and the fact that $\Lambda_{ab}^{2}/\Lambda_{c}^{2}$ and Λ_{ab}^{2}/s_{ab} are non-universal quantities of order 1. The non-universality of Λ_{ab}^{2}/s_{ab} clearly emerges from the data for $Pr_{2-x}Ce_xCuO_{4-\delta}$ displayed in Fig. 9b, pointing to $1/\lambda_{ab}^{2}(0) = 2.5\ 10^{-5}\ T_c/\rho_{ab}$ (dashed line) in contrast to $1/\lambda_{ab}^{2}(0) = 5.2\ 10^{-5}\ T_c/\rho_{ab}$ (solid line).

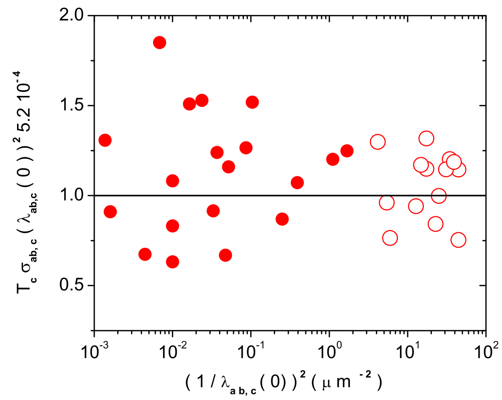

FIG. 10. $\lambda_{ab,c}^{2}(0)\,T_c\sigma_{ab,c}^{dc}\ 5.210^{-4}$ *vs.* $1/\ \lambda_{ab,c}^{2}(0)$ for the data shown in Fig. 5. • : c-axis; ◯: *ab*-plane.

In any case, the overall impressive evidence for anisotropic 3D-XY scaling raises again serious doubts that 2D models [19] are potential candidates to explain superconductivity in the cuprates. Indeed, the doping or T_c dependence of the c-axis correlation length is an essential ingredient (see Figs. 5a, Fig. 7b and Fig. 9a). Furthermore, since both, $1/\lambda_{ab}^{2}(0)$ and $1/\lambda_{c}^{2}(0)$ tend to zero by approaching 2D-QSI criticality, this plot also uncovers the flow to this quantum critical point, as indicated by the arrow in Fig. 3.

Having established the remarkable reliability of the scaling relations (18) and (20) we are now prepared to discuss the isotope effects on T_c and the zero temperature in-plane penetration depth. Since Eq. (5) is universal, it also implies that the changes ΔT_c, Δd_s and $\Delta\left(1/\lambda_{ab}^{2}(T=0)\right)$, induced by pressure or isotope exchange are not independent, but close to 2D-QSI criticality related by [52]

$$\frac{\Delta T_c}{T_c} + 2\frac{\Delta\left(\lambda_{ab}(0)\right)}{\lambda_{ab}(0)} = \frac{\Delta d_s}{d_s}, \tag{22}$$

while the approximate scaling relation (18), applicable over an extended doping range (see Fig. 3) yields

$$\frac{\Delta T_c}{T_c} + 2\frac{\Delta\left(\lambda_{ab}(0)\right)}{\lambda_{ab}(0)} = \frac{\Delta\left(\xi_{c0}/\Lambda_{ab}^{2}\right)}{\left(\xi_{c0}/\Lambda_{ab}^{2}\right)}, \tag{23}$$

where according to relation (18)

$$\frac{\xi_{c0}}{\Lambda_{ab}^{2}} = \frac{16\pi^3 k_B}{\Phi_0^2 f}\lambda_{ab}^{2}(0)\,T_c. \tag{24}$$

Approaching 2D-QSI criticality matching requires $\Delta\left(\xi_{c0}/\Lambda_{ab}^{2}\right)/\left(\xi_{c0}/\Lambda_{ab}^{2}\right) \rightarrow \Delta d_s/d_s$. For the oxygen isotope effect (^{16}O vs. ^{18}O) on a physical quantity X the relative isotope shift is defined as $\Delta X/X = (^{18}X -^{16}X)/^{18}X$. In this case the effect has been traced back to a change of the critical amplitude of the c-axis correlation length upon oxygen isotope exchange. Another implication is that the absence of a substantial isotope effect on the transition temperature, e.g. close to optimum doping, is not of particular significance. In this case what is left is the effect on the in-plane penetration depth.

In Fig. 11 we show the data for the oxygen isotope effect in $La_{2-x}Sr_xCuO_4$ [64,65], $Y_{1-x}Pr_xBa_2Cu_3O_{7-\delta}$ [65–67] and $YBa_2Cu_3O_{7-\delta}$ [65,68], extending from the underdoped to the optimally doped regime, in terms of $\Delta\left(\lambda_{ab}(0)\right)/$

$\lambda_{ab}(0)$ versus $\Delta T_c/T_c$. It is evident that there is a correlation between the isotope effect on T_c and $\lambda_{ab}(0)$. Indeed, approaching the 2D-QSI transition, as marked by the arrow, the data tends to fall on the straight line, which is Eq. (22). This yields for the isotope effect on d_s the estimate $\Delta d_s/d_s = 3.3(4)\%$. Approaching optimum doping, this contribution renders the isotope effect on T_c considerably smaller than that on $\lambda_{ab}(0)$. In fact, even in nearly optimally doped $YBa_2Cu_3O_{7-\delta}$, where $\Delta T_c/T_c = -0.26(5)\%$, a substantial isotope effect on the in-plane penetration depth, $\Delta\lambda_{ab}(0)/\lambda_{ab}(0) = -2.8(1.0)\%$, has been established by direct observation, using the novel low-energy muon-spin rotation technique [68].

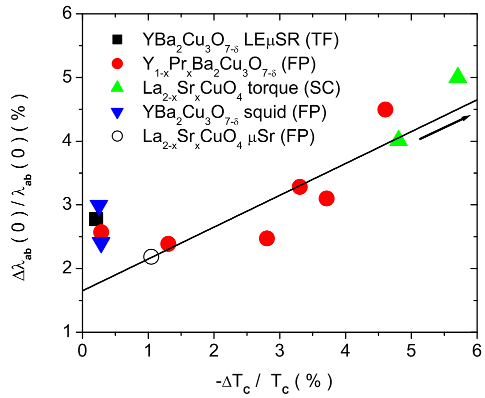

FIG. 11. Data for the oxygen isotope effect in underdoped $La_{2-x}Sr_xCuO_4$(◯: x=0.15 [65], ▲: x=0.08, 0.086 [64]), $Y_{1-x}Pr_xBa_2Cu_3O_{7-\delta}$ (•: x=0, 0.2, 0.3, 0.4 [65–67]) and $YBa_2Cu_3O_{7-\delta}$ (▼ [65], ■ [68]) in terms of $\Delta(\lambda_{ab}(0))/\ \lambda_{ab}(0)$ versus -$\Delta T_c/T_c$. In the direction of the arrow the solid line indicates the flow to 2D-QSI criticality and provides with Eq. (22) an estimate for the oxygen isotope effect on d_s, namely $\Delta d_s/d_s = 3.3(4)\%$.

Fig. 11 also shows that away from 2D-QSI criticality the experimental data does no longer fall onto the straight line. Since in the underdoped regime $\Delta\left(\xi_{c0}/\Lambda_{ab}^2\right)/\left(\xi_{c0}/\Lambda_{ab}^2\right) \rightarrow \Delta d_s/d_s$ this behavior unfolds according to Eq. (23) the doping dependence of $\Delta\left(\xi_{c0}/\Lambda_{ab}^2\right)/\left(\xi_{c0}/\Lambda_{ab}^2\right)$. To disentangle the doping dependence of $\Delta\left(\xi_{c0}/\Lambda_{ab}^2\right)$ and ξ_{c0}/Λ_{ab}^2 we displayed in Fig. 12a $\Delta T_c/T_c + 2\Delta(\lambda_{ab}(0))/\ \lambda_{ab}(0)$ *vs.* x for the oxygen isotope in $La_{2-x}Sr_xCuO_4$. For comparison we included $1/\xi_{c0} \propto 1/\left(T_c\lambda_{ab}^2(0)\right)$ *vs.* x, indicating that $\Delta T_c/T_c + 2\Delta(\lambda_{ab}(0))/\ \lambda_{ab}(0)$ scales as $1/\xi_{c0} \propto 1/\left(T_c\lambda_{ab}^2(0)\right)$and accordingly $\Delta\xi_{c0}/\xi_{c0}$ as $\Delta\xi_{c0}/\xi_{c0} \propto 1/\xi_{c0}$. Hence $\Delta\xi_{c0}$ is essentially independent of the dopant concentration.

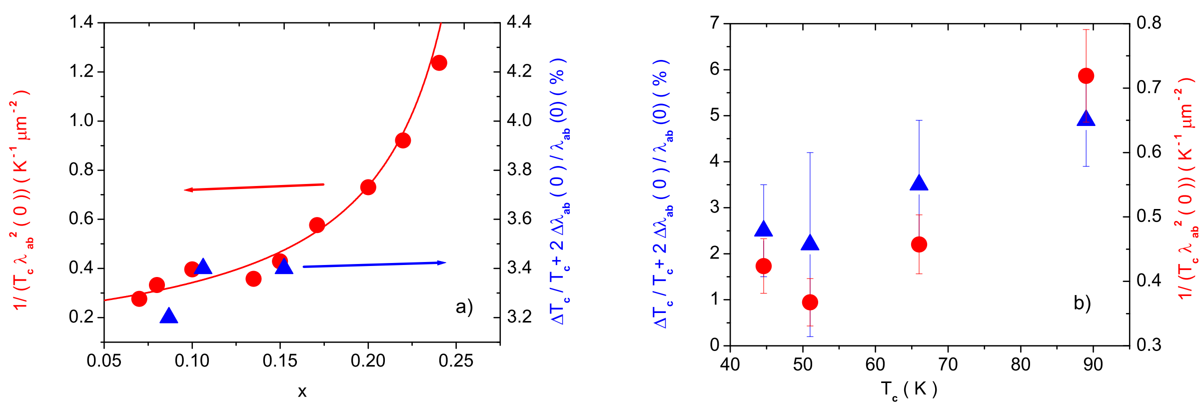

FIG. 12. a) Data for the oxygen isotope effect in $La_{2-x}Sr_xCuO_4$(▲ : x= 0.086 [64], x=0.105 [65], 0.15 [69] in terms of $\Delta T_c/T_c + 2\Delta(\lambda_{ab}(0))/\ \lambda_{ab}(0)$ *vs.* x. For comparison we included the experimental data (•) for $1/\xi_{c0} \propto 1/\left(T_c\lambda_{ab}^2(0)\right)$ *vs.* x and the solid curve is taken from Eq. (12). b) $\Delta T_c/T_c + 2\Delta(\lambda_{ab}(0))/\ \lambda_{ab}(0)$ *vs.* T_c of $Y_{1-x}Pr_xBa_2Cu_3O_{7-\delta}$ (▲: x=0, 0.2, 0.3, 0.4) [56,70]. The experimental data (•) for $1/\xi_{c0} \propto 1/\left(T_c\lambda_{ab}^2(0)\right)$*vs.* T_c are included for comparison.

Clearer evidence for this scaling behavior of the isotope effect on the amplitude of the c-axis correlation length emerges from Fig. 12b showing $\Delta T_c/T_c + 2\Delta(\lambda_{ab}(0))/\ \lambda_{ab}(0)$ *vs.* T_c and $1/\xi_{c0} \propto 1/\left(T_c\lambda_{ab}^2(0)\right)$*vs.* T_c for

$Y_{1-x}Pr_xBa_2Cu_3O_{7-\delta}$. This opens a window onto the origin of the unconventional isotope effects in the cuprates. Indeed, there is the evidence for a nearly linear doping dependence of ξ_{c0}, namely $\xi_{c0} \approx d_s - b\delta$ (see Eq.(12)) and Figs. 5a, 6 and 9a) and the limiting behavior $\Delta\xi_{c0} \rightarrow \Delta d_s$ (Eq. (16). To substantiate this point we displayed in Fig. 13 the experimental data for $Y_{1-x}Pr_xBa_2Cu_3O_{7-\delta}$ in terms of $T_c\lambda_{ab}^2(0)$ *vs.* T_c [56] and $\rho_{ab}(T_c^+)$ *vs.* T_c [71,72]. Apparently, the scaling relations (19) and (20), requiring $\xi_{c0} \propto T_c\lambda_{ab}^2(0) \propto \rho_{ab}(T_c^+)$ are well confirmed.

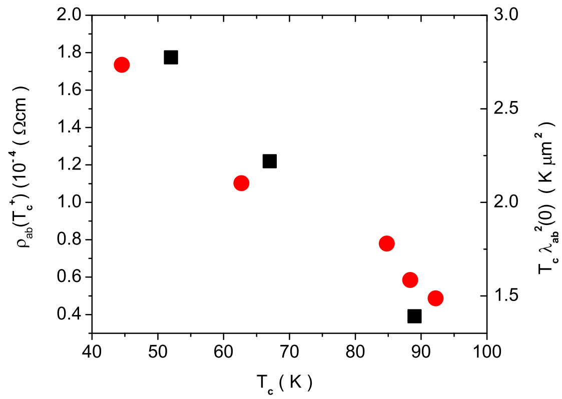

FIG. 13. $T_c\lambda_{ab}^2(0)$ *vs.* T_c for $Y_{1-x}Pr_xBa_2Cu_3O_{7-\delta}$ taken from [56] and $\rho_{ab}(T_c^+)$ *vs.* T_c taken from Maple *et al.* [71] and Dalichaouch *et al.* [72].

Together with the weak doping dependence of $\Delta\xi_{c0}$ resulting from the evidence for $\Delta\xi_{c0}/\xi_{c0} \propto 1/\xi_{c0}$(Fig. 12b) these constraints imply that

$$\Delta\xi_{c0} \approx \Delta d_s - \Delta b\delta^n - bn\delta^{n-1}\Delta\delta = \Delta d_s + bn\delta^{n-1}\Delta x_u,\ n \gtrsim 1, \tag{25}$$

where $\delta = x - x_u$ is the concentration of the mobile charge carriers. To appreciate the implications it is instructive to consider the phase diagram of $La_{2-x}Sr_xCuO_4$ displayed in Fig.14.

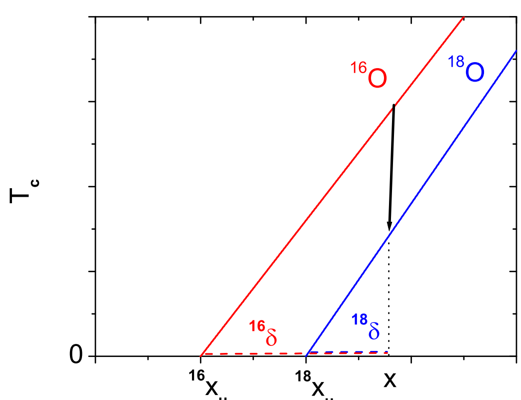

FIG. 14. Schematic sketch of the oxygen isotope effect on the phase diagram of $La_{2-x}Sr_xCuO_4$ close to the underdoped limit where the 2D-QSI transition occurs. The solid lines are the phase transition lines $T_c(x)$. Since the magnitude of $\Delta T_c =^{16} T_c -^{18} T_c$ increases with reduced x the underdoped limit shifts from $^{16}x_u$ to $^{18}x_u$. The arrow at fixed x indicates the reduction of T_c upon complete oxygen isotope exchange ($^{16}O \rightarrow ^{18}O$) and the dashed lines the mobile carrier concentration $^{16,18}\delta = x -^{16,18} x_u$.

Given the experimental fact that x and the lattice constants do not change upon complete oxygen isotope exchange ($^{16}O \rightarrow ^{18}O$) [54,55], while T_c is lowered and ΔT_c increases by approaching the underdoped limit, it follows that this limit shifts from $^{16}x_u$ to $^{18}x_u$. Hence, for fixed x $La_{2-x}Sr_xCuO_4$ becomes in the interval $^{16}x_u < x < ^{18}x_u$ an insulator and the shift of the underdoped limit from $^{16}x_u$ to $^{18}x_u$ leads to a reduction of the concentration δ of the mobile charge carriers, as indicated in Fig. 14. The lesson then is, the unconventional isotope effects in the cuprates stem

from the shifts of d_s and the underdoped limit x_u. Since the volume of the unit cell is preserved this changes imply local lattice distortions. Consequently, the isotope shifts of T_c and $\lambda_{ab}(0)$ are not related by scaling relations imposed by 3D-XY universality only, but reveal the existence and relevance of the coupling between the superfluid and volume preserving local lattice distortions.

This lesson appears to contradict interpretations based on the London formula [73]

$$\frac{1}{\lambda_{ii}^2(0)} = \frac{4\pi n_s e^2}{m_{ii}^* c^2}, \tag{26}$$

where n_s is the number density of the superfluid and m_{ii}^* the effective mass of the pairs in direction i. There is the experimental evidence that the lattice constants do not change upon complete oxygen isotope exchange (^{16}O $\rightarrow$ ^{18}O) [54,55]. Furthermore, recent nuclear quadrupole resonance (NQR) studies of ^{16}O and ^{18}O substituted optimally doped $YBa_2Cu_3O_{7-\delta}$ powder samples revealed that the change of the total charge density caused by the isotope exchange is less than 10^{-3} [68]. These experimental facts have then be taken as evidence for a negligibly small isotope effect on n_s [68]. However, in general the London relation is just a way of parameterizing experimental results, with no discernible connection to the carrier concentration or, e.g. the band mass. Indeed, even in conventional superconductors $1/\lambda_{ii}^2(0)$ is determined by normal state properties, namely the integral of the Fermi velocity over the Fermi surface. In the special case of spherical and ellipsoidal Fermi surfaces one recovers Eq. (26) in the form, $1/\lambda_{ii}^2(T=0) = 4\pi n e^2/\left(m_{ii}^* c^2\right)$, where n is the number density of the electrons in the normal state and m_{ii}^* the band mass [74]. In any case, since the Hall effect is related to the concentration of mobile charge carriers [75] the reduction of δ upon isotope exchange should lead to an isotope effect on the Hall constant R_H. Within the framework of the model proposed by Stojkovic and Pines [76], where both the resistivity and the Hall constant are inversely proportional to δ, the relative isotope shifts are then related by

$$\frac{\Delta R_H}{R_H} = \frac{\Delta \rho}{\rho} = -\frac{\Delta \delta}{\delta}. \tag{27}$$

Although qualitative evidence for the oxygen isotope effect on the resistivity emerges from the measurements on $Y_{1-x}Pr_xBa_2Cu_3O_{7-\delta}$ [77] and on Pr-, Ca-, and Zn-substituted $YBa_2Cu_3O_{7-\delta}$ [78], this relationship awaits to be tested quantitatively.

Further evidence for this coupling emerges from the combined isotope and finite size effects. Recently, it has been shown that the notorious rounding of the superconductor to normal state transition is fully consistent with a finite size effect, revealing that bulk cuprate superconductors break into nearly homogeneous superconducting grains of rather unique extent [14,46,47,56]. A characteristic feature of this finite size effect on the temperature dependence of the in-plane penetration depth λ_{ab} is the occurrence of an inflection point giving rise to an extremum in $d\left(\lambda_{ab}^2(T=0)/\lambda_{ab}^2(T)\right)/dT$ at T_{p_c}. Here $\lambda_{ab}^2(T_{p_c})$, T_{p_c} and the length L_c of the grains along the c-axis are related by [46,47,56]

$$\frac{1}{\lambda_{ab}^2(T_p)} = \frac{16\pi^3 k_B T_{p_c}}{\Phi_0^2 L_c}. \tag{28}$$

Recently, the effect of oxygen isotope exchange on L_c has been studied in $Y_{1-x}Pr_xBa_2Cu_3O_{7-\delta}$ [56]. Note that the relative shifts of $\lambda_{ab}^2(T_{p_c})$, T_{p_c} and L_c are not independent but according to Eq. (28) related by

$$\frac{\Delta L_c}{L_c} = \frac{\Delta T_{p_c}}{T_{p_c}} + \frac{\Delta \lambda_{ab}^2(T_{p_c})}{\lambda_{ab}^2(T_{p_c})} = \frac{\Delta T_{p_c}}{T_{p_c}} + 2\frac{\Delta \lambda_{ab}(T_{p_c})}{\lambda_{ab}(T_{p_c})}, \tag{29}$$

which is just the finite size scaling counterpart of Eq.(23). Some estimates resulting from the finite size scaling analysis are listed in Table I. Several observations emerge. First, the spatial extent of the homogeneous domains L_c changes upon isotope exchange (^{16}O, ^{18}O). To appreciate the implications of this observation, we note again that for fixed Pr concentration the lattice parameters remain essentially unaffected [54,55]. Accordingly, an electronic mechanism, without coupling to local lattice distortions implies $\Delta L_c = 0$. On the contrary, a significant change of L_c upon oxygen exchange requires local lattice distortions involving the oxygen lattice degrees of freedom and implies with Eq. (29) a coupling between these distortions and the superfluid, probed by $\lambda_{ab}(T_{p_c})$. Second, since the relative shift of T_{p_c} is very small the change of L_c is essentially due to the superfluid, probed by $\lambda_{ab}(T_{p_c})$. Third, L_c increases systematically with reduced T_{p_c}.

x	0	0.2	0.3
$\Delta L_c/L_c$	0.12(5)	0.13(6)	0.16(5)
$\Delta T_{p_c}/T_{p_c}$	-0.000(2)	-0.015(3)	-0.021(5)
$\Delta\lambda_{ab}^2\left(T_{p_c}\right)/\lambda_{ab}^2\left(T_{p_c}\right)$	0.11(5)	0.15(6)	0.15(5)
$^{16}T_{p_c}$(K)	89.0(1)	67.0(1)	52.1(1)
$^{16}L_c$(Å)	9.7(4)	14.2(7)	19.5(8)
$^{16}\lambda_{ab}\left(0\right)$(Å)	1250(10)	1820(20)	2310(30)

Table I: Finite size estimates for the relative changes of L_c, T_{p_c} and $\lambda_{ab}^2\left(T_{p_c}\right)$ upon oxygen isotope exchange for $Y_{1-x}Pr_xBa_2Cu_3O_{7-\delta}$ [56]. We have seen that the unconventional isotope shifts of T_c , $\lambda_{ab}\left(0\right)$ and L_c are not related by

scaling relations imposed by 3D-XY universality only, but reveal the existence and relevance of the coupling between the superfluid and volume preserving local lattice distortions. Their response to isotope exchange shifts d_s, L_c and the underdoped limit x_u, accompanied by a reduction of the concentration δ of mobile carriers. These observations contradict the majority opinion on the mechanism of superconductivity in the cuprates that it occurs via a purely electronic mechanism involving spin excitations, and the lattice degrees of freedom are irrelevant.

As aforementioned the exact 3D-XY scaling relation (17) and its approximate counterpart (18) should also apply when pressure is applied. As does the isotope effect, there is a generic decrease of T_c with pressure in simple-metal superconductors (Sn, Al, In, *etc.*). In cuprate superconductors the situation is considerably more complex because changes in both the local lattice distortions and lattice constants occur, and there are pressure-induced relaxation phenomena. In $YBa_2Cu_3O_{7-\delta}$ [79,80], $Tl_2Ba_2CuO_{6+\delta}$ [81–83], and other cuprates [84] the initial dependence of T_c on pressure often depends markedly on the pressure-temperature history of the sample. The relaxation phenomena responsible for this behavior are believed to originate from pressure-induced ordering of mobile oxygen defects in the lattice and the value of T_c appears to be a sensitive function of both the concentration and the arrangement of these defects. To avoid these difficulties we concentrate on $YBa_2Cu_4O_8$, exhibiting a spectacular increase of T_c under pressure by nearly 30K [85,86]. Furthermore, the pressure dependence of the critical amplitude λ_{ab0} have been studied as well [57]. The data displayed in Fig. 15a show that the pressure dependencies of T_c and $1/\ \lambda_{ab0}^2$ are initially nearly linear and positive, as indicated by the solid and dashed lines given by

$$T_c\left(p\right) = 79.07 + 0.5p,\ \ 1/\lambda_{ab0}^2\left(p\right) = 33 + 1.5p. \tag{30}$$

As a result both $\Delta T_c/T_c$ and $\Delta\left(1/\lambda_{ab0}^2\right)/\left(1/\lambda_{ab0}^2\right) = -2\Delta\lambda_{ab0}/\lambda_{ab0}$ are positive and increase with pressure, as shown in Fig. 15b. This differs from the oxygen isotope effect where these quantities are negative (see Fig. 11). Nevertheless, the universal relation (17) implies that these pressure induced changes are not independent but related by

$$\frac{\Delta T_c}{T_c} + 2\frac{\Delta\lambda_{ab0}}{\lambda_{ab0}} = \frac{\Delta\xi_{c0}}{\xi_{c0}}. \tag{31}$$

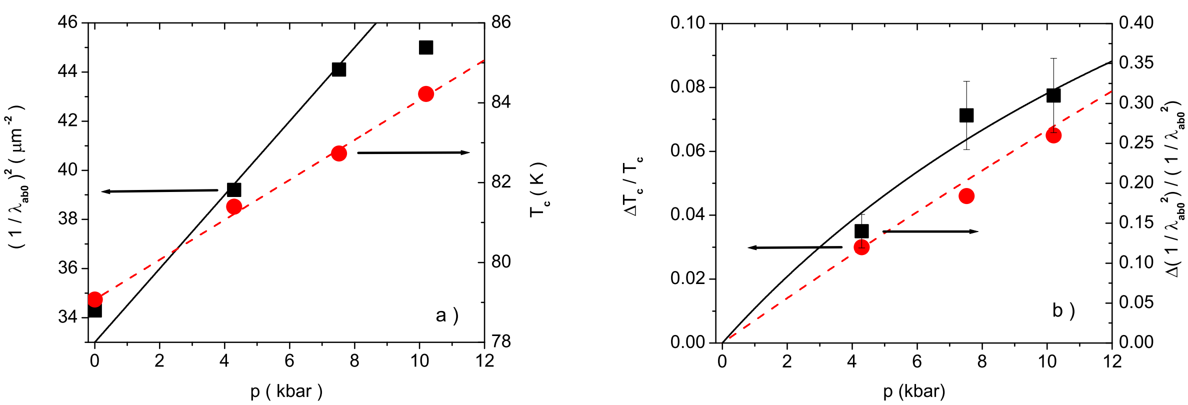

FIG. 15. a) Pressure dependence of T_c and $1/\ \lambda_{ab0}^2$ in $YBa_2Cu_4O_8$ taken from Khasanov *et al.* [57]. The dashed and solid lines are given by Eq. (30). b) Pressure dependence of $\Delta T_c/T_c$ and $\Delta\left(1/\lambda_{ab0}^2\right)/\left(1/\lambda_{ab0}^2\right) = -2\Delta\lambda_{ab0}/\lambda_{ab0}$. The solid and dashed lines follow from Eq. (30).

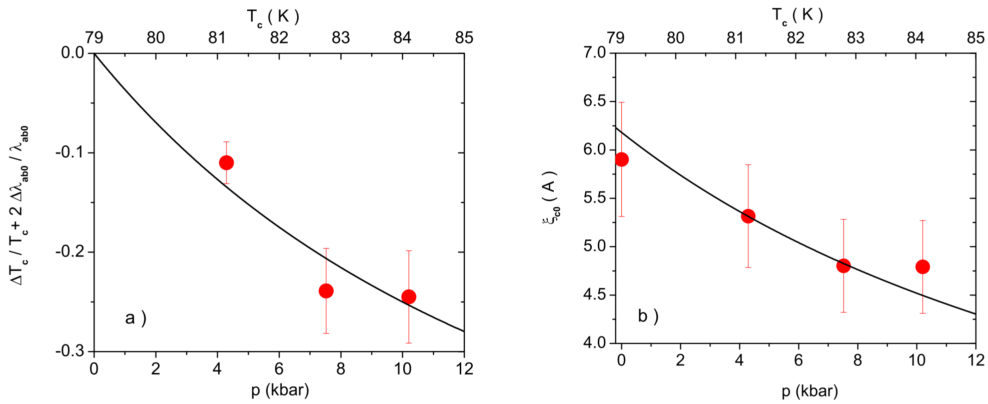

FIG. 16. a) $\Delta T_c/T_c + 2\Delta\lambda_{ab0}/\lambda_{ab0}$ *vs.* p and T_c for $YBa_2Cu_4O_8$ derived from the data of Khasanov *et al.* [57]. The solid line follows from Eq. (30); b) ξ_{c0} *vs.* p and T_c for $YBa_2Cu_4O_8$ derived from the data of Khasanov *et al.* [57] with the aid of Eq. (9). The solid line follows from Eqs. (17) and (30).

In Fig. 16a we displayed the experimental estimates for $\Delta T_c/T_c+2\Delta\lambda_{ab0}/\lambda_{ab0}$ *vs.* p and T_c for $YBa_2Cu_4O_8$ derived from the data of Khasanov *et al.* [57]. For comparison we included the behavior resulting from Eq. (30). To interpret the data we invoke Eq. (9) to derive from $T_c\,(p)$ and $\lambda_{ab0}\,(p)$ the pressure dependence of $\xi_{c0}\,(p)$. A glance to Fig. 16b shows that ξ_{c0} decreases with increasing pressure and transition temperature. Noting that $YBa_2Cu_4O_8$ falls at zero pressure into the slightly underdoped regime this behavior can be compared with the T_c dependence of ξ_{c0} in underdoped $La_{2-x}Sr_xCuO_4$ displayed in Fig. 5a. In this regime the rise of T_c implies a reduction of ξ_{c0}. Considering the behavior in the (ξ_{c0}, T_c)- plane the hydrostatic pressure effect may then also be viewed as an inverse oxygen isotope effect ($^{18}O \rightarrow {}^{16}O$), a pressure induced crossover to less anisotropic 3D behavior, or a crossover to optimum doping. This crossover is also related to the initial decrease of the a-Lattice constant under applied hydrostatic pressure [87]. Thus, we arrive at the following tentative scenario. If the layer is originally underdoped hydrostatic pressure enhances T_c and reduces both λ_{ab0} and ξ_{c0}; if it is overdoped, it decreases T_c increases λ_{ab0} and reduces ξ_{c0}. This behavior can be anticipated from from Figs. 5a, 15 and 16 and uncovers again 3D-XY scaling and 2D to 3D crossover to be at work.

So far we concentrated on scaling relations emerging from the universal amplitude combination (17). There is a multitude of other combinations including the relation between magnetization, applied magnetic field and T_c [14,88], as well as the universal relation between the critical amplitude $A^+$of the specific heat singularity and the correlation volume V_c^+ [14,42]

$$A^+V_c^+ = \left(R^+\right)^3, V_c^+ = \xi_{a0}\xi_{b0}\xi_{c0}. \tag{32}$$

α is the critical exponent and $A^\pm$ the critical amplitude of the specific heat singularity, $c = \left(A^\pm/\alpha\right)|t|^{-\alpha} + B^\pm$, where $\pm = sgn(T/T_c - 1)$. 3D-XY universality implies [42]

$$\frac{A^+}{A^-} = 1.07, \quad R^+ = 0.361, \ \alpha = 2 - 3\nu = -0.013, \ \nu = 0.671. \tag{33}$$

Although the singular part of the specific heat is small compared to the phonon contribution and inhomogeneities set limits in exploring the critical regime [14,46] the measurements on nearly optimally doped $YBa_2Cu_3O_{7-\delta}$ [14,89] and $La_{2-x}Sr_xCuO_4$ [90] point clearly to 3D-XY critical behavior. Experimentally it is well established that the specific heat anomaly and with that the critical amplitude A^+ decreases dramatically by approaching the underdoped limit (2D-QSI criticality) [91–93]. Since $V_c^+ = \xi_{a0}\xi_{b0}\xi_{c0} \approx \gamma_{T_c}^2\xi_{c0}^3$ and $\xi_{c0} \rightarrow d_s$ (see Figs. 4, 5a and 7b) while $\gamma_{T_c}^2 \rightarrow \infty$ (see Eq. (2)) in the underdoped limit, this behavior is a consequence of the 3D-2D-crossover. Furthermore, combining the universal 3D-XY amplitude combinations (17) and (32) we obtain the universal relation

$$A^+ = \frac{\left(R^+\right)^3}{\left(\gamma_{T_c}\right)^2 \xi_{c0}^3} = \left(\frac{\Phi_0^2 f}{16\pi^3 k_B}\right)^3 \frac{1}{\gamma_{T_c}^2 \lambda_{ab0}^6 T_c^3}, \tag{34}$$

relating the critical amplitudes of specific heat, anisotropy, in-plane penetration depth and anisotropy. Consequently, the pressure and isotope effects on these quantities are not independent but related by [53]

$$\frac{\Delta A^{+}}{A^{+}}=-2\frac{\Delta\gamma_{T_c}}{\gamma_{T_c}}-6\frac{\Delta\lambda_{ab0}}{\lambda_{ab0}}-3\frac{\Delta T_c}{T_c}. \tag{35}$$

Although these universal 3D-XY relations await to be tested experimentally they reveal again that as long as uncharged fluctuations dominate these effects do not change T_c only but uncover the coupling between energy- and superfluid fluctuations. To illustrate the dramatic decrease of the specific heat anomaly in the underdoped regime we plotted in Fig. 17 $1/\left(\gamma_{T=0}^{2}T_c^{3}\lambda_{ab}^{6}(0)\right)$ *vs.* T_c for $YBa_2Cu_3O_{7-\delta}$ derived from the data of Trunin and Nefyodov [94]. In the heavily underdoped regime where $T_c\propto 1/\lambda_{ab}^{2}(0)$ (see Eq. (5)) the magnitude of A^{+} is then manly controlled by the anisotropy γ which diverges at 2D-QSI criticality (see Eq. (2) and Figs. 1b and 2)

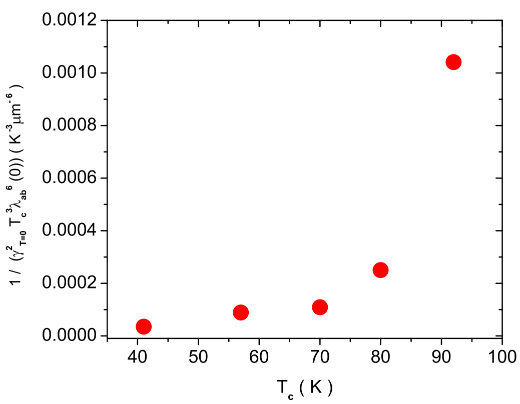

FIG. 17. $1/\left(\gamma_{T=0}^{2}T_c^{3}\lambda_{ab}^{6}(0)\right)$ *vs.* T_c for $YBa_2Cu_3O_{7-\delta}$ derived from the data of Trunin and Nefyodov [94].

Another example is the universal relation between magnetization m, applied magnetic field H and T_c [7,14],

$$m_c=\frac{Q_3C_3k_B}{\Phi_0^{3/2}}H_cT_c\gamma_{T_c},\ m_{ab}=\frac{Q_3C_3k_B}{\Phi_0^{3/2}}H_{ab}\frac{T_c}{\gamma_{T_c}}, \tag{36}$$

for fields applied parallel (H_c) or perpendicular (H_{ab}) to the c-axis. Q_3C_3 is a universal constant [7,14]. Hence, the isotope and pressure effects on these quantities are not independent but related by

$$\frac{\Delta m_c}{m_c}=\frac{\Delta T_c}{T_c}+\frac{\Delta\gamma_{T_c}}{\gamma_{T_c}},\ \frac{\Delta m_{ab}}{m_{ab}}=\frac{\Delta T_c}{T_c}-\frac{\Delta\gamma_{T_c}}{\gamma_{T_c}}. \tag{37}$$

Although the isotope effect on the magnetization is well established [64,66,77,78] these relationships await to be explored.

In summary, by taking experimental data for T_c, $\lambda_{ab,c}(0)$, $\sigma_{ab,c}^{dc}(T_c^{+})=1/\rho_{ab,c}^{dc}(T_c^{+})$, $\gamma=\lambda_c/\lambda_{ab}$ of a variety of cuprates encompassing the underdoped and overdoped regimes, we have shown that these quantities are not independent but related by scaling relations reminiscent to anisotropic systems falling into the 3D-XY universality class. They differ from the exact scaling relation by the ratio between the critical amplitudes of the penetration depths and their zero temperature counterparts. However, the remarkable agreement revealed that the doping and family dependence of this ratio is rather weak. As the unconventional isotope effects are concerned, the rather sparse experimental data turned out to be consistent with the 3D-XY scaling relations, connecting the isotope effects on T_c, $\lambda_{ab}(0)$ and the c-axis correlation length ξ_c. Guided by the doping dependence of ξ_c we have shown that the oxygen isotope effects are associated with a change of d_s, a shift of the underdoped limit and a reduction of the concentration of mobile carriers. Since ξ_c scales as $\xi_c\propto\rho_{ab}(T_c^{+})=1/\sigma_{ab}(T_c^{+})$ we obtained the approximate 3D-XY scaling relation (4). It connects the relative isotope shifts of measurable properties and awaits together with Eq. (27), relating the shifts of Hall constant, resistivity and mobile carrier concentration upon oxygen isotope exchange, to be tested quantitatively. Qualitative evidence for the oxygen isotope effect on the resistivity emerges from the measurements on $Y_{1-x}Pr_xBa_2Cu_3O_{7-\delta}$ [77] and on Pr-, Ca-, and Zn-substituted $YBa_2Cu_3O_{7-\delta}$ [78]. Furthermore, we have seen that the combined isotope and finite size effects open a door to probe the coupling between local lattice distortions and superconductivity in terms of the isotope shift of L_c, the spatial extent of the homogeneous superconducting grains along the c-axis. Noting that $\Delta L_c/L_c$ is rather large (see Table I) this change revealed the coupling between superfluidity and local lattice distortion and this coupling is likely important in understanding the pairing mechanism.

Further evidence for 3D-XY scaling to be at work emerged from the effects of hydrostatic pressure on T_c and $\lambda_{ab}(0)$, as well as from the doping dependence of the specific heat singularity. Although the currently available experimental data of the pressure and isotope effects, as well as on the critical amplitudes are rather sparse, we have shown that a multitude of empirical correlations between T_c, magnetic penetration lengths, resistivity, conductivity, specific heat, *etc.* are fully consistent with the universal critical amplitude combinations for anisotropic systems falling into the 3D-XY universality class and undergo a crossover to a 2D quantum superconductor to insulator transition (2D-QSI). Not unexpectedly we have shown that these correlations are controlled by the doping or T_c dependence of the c-axis correlation length ξ_c and the anisotropy γ_T. Although much experimental work remains to be done, measuring the quantities of interest on the same sample, the remarkable consistency with 3D-XY scaling and the crossover to the 2D-QSI quantum critical point single out 3D and anisotropic microscopic models which incorporate local lattice distortions, fall in the experimentally accessible regime into the 3D-XY universality class, and incorporate the crossover to 2D-QSI criticality where superconductivity disappears.

ACKNOWLEDGMENTS

The author is grateful to D. Di Castro, S. Kohout and J. Roos for very useful comments and suggestions on the subject matter and J. M. Triscone for pertinent advice concerning the Hall effect.

---

[1] M. Suzuki and M. Hikita, Phys. Rev. B **44**, 249 (1991).
[2] Y. Nakamura and S. Uchida, Phys. Rev. Phys. Rev. **B** 47, 8369 (1993).
[3] Y. Fukuzumi, K. Mizuhashi, K. Takenaka, and S. Uchida, Phys. Rev. Lett. **76**, 684 (1996).
[4] M. Willemin, C. Rossel, J. Hofer, H. Keller, and A. Revcolevschi, Phys. Rev. B **59**, 717 (1999).
[5] T. Kimura, K. Kishio, T. Kobayashi, Y. Nakayama, N. Motohira, K. Kitazawa, and K. Yamafuji, Physica C **192,** 247 (1992).
[6] T. Sasagawa, Y. Togawa, J. Shimoyama, A. Kapitulnik, K. Kitazawa, and K. Kishio, Phys. Rev. B **61**, 1610 (2000).
[7] J. Hofer, T. Schneider, J. M. Singer, M. Willemin, H. Keller, T. Sasagawa, K. Kishio, K. Conder, and J. Karpinski, Phys. Rev. B **62,** 631 (2000).
[8] T. Shibauchi, H. Kitano, K. Uchinokura, A. Maeda, T. Kimura, and K. Kishio, Phys. Rev. Lett. **72**, 2263 (1994).
[9] C. Panagopoulos, J. R. Cooper, T. Xiang, Y. S. Wang and C. W. Chu, Phys. Rev. B **61**, 3808 (2000).
[10] J. L. Tallon, C. Bernhard, H. Shaked, R. L. Hitterman, and J. D. Jorgensen, Phys. Rev. B **51**, 12911 (1995).
[11] M. R. Presland, J. L. Tallon, R. G. Buckley, R. S. Liu, and N. E. Flower, Physica C **176**, 95 (1991).
[12] N. Momono, M. Ido, T. Nakano, M. Oda, Y. Okajima, and K. Yamaya, Physica C **233**, 395 (1994).
[13] T. Schneider, Acta Physica Polonica A **91,** 203 (1997).
[14] T. Schneider and J. M. Singer, *Phase Transition Approach To High Temperature Superconductivity*, Imperial College Press, London, 2000.
[15] T. Schneider and J. M. Singer, J. of Superconductivity **13**, 789 (2000).
[16] T. Schneider, in *The Physics of Superconductors*, edited by K. Bennemann and J. B. Ketterson (Springer, Berlin 2004) p. 111.
[17] L. Onsager, Phys. Rev. **65**, 117 (1944).
[18] T. Schneider, Physica B **326**, 289 (2003).
[19] P. W. Anderson, P. A. Lee, M. Randeria, T. M. Rice, N. Trivedi, and F. C. Zhang, cond-mat/0311467.
[20] J. Hofer, J. Karpinski, M. Willemin, G.I. Meijer, E.M. Kopnin, R. Molinski, H. Schwer, C. Rossel, and H. Keller, Physica C **297**, 103 (1998).
[21] G. Xiao, M. Z. Cieplak, J. Q. Xiao, and C. L. Chien, Phys. Rev. B **42**, 8752 (1990).
[22] J. M. Tarascon *et al.*, Phys. Rev. B **42**, 218 (1990).
[23] S. Watauchi, H. Ikuta, H. Kobayashi, J. Shimoyama, and K. Kishio, Phys.Rev. B **64**, 64520 (2001).
[24] T. R. Chien, W. R. Datars, B. W. Veal, A. P. Paulikas, P. Kostic, Chun Gu and Y. Jiang, Physica C **229**, 273 (1994).
[25] T. R. Chien, W. R. Datars, M. D. Lan, J. Z. Liu, and R. N. Shelton, Phys. Rev. B **49**, 1342 (1994).
[26] T. R. Chien and W. R. DatarsJ. Z. Liu, M. D. Lan, and R. N. Shelton, Physica C **221**, 428 (1994).
[27] X. F. Sun, X. Zhao, X.-G. Li, and H. C. Ku, Phys. Rev. B **59**, 8978 (1999).
[28] C. Panagopoulos, J. R. Cooper, N. Athanassopoulou, and J. Chrosch, Phys. Rev. B **54**, 12721 (1996).
[29] C. C. Homes, S. V. Dordevic, M. Strongin, D. A. Bonn, Ruixing Liang, W. N. Hardy, Seiki Koymia, Yoichi Ando, G. Yu, X. Zhao, M. Greven, D. N. Basov, and T. Timusk, cond-mat/0404216.

[30] D. N. Basov *et al.*, Phys. Rev. Lett. **74**, 598 (1995).
[31] C. C. Homes *et al.*, Phys. Rev. B **60**, 9782 (1999).
[32] H. L. Liu *et al.*, J. Phys: Condens. Matter **11**, 239 (1999).
[33] D.N. Basov, T. Timusk, B. Dabrowski, and J. D. Jorgensen, Phys. Rev. B **50**, 3511 (1994).
[34] C. C. Homes, T. Timusk, D. A. Bonn, R. Liang, and W. N. Hardy, Physica C **254**, 265 (1995).
[35] J. Schützmann, S. Tajima, S. Miyamoto, and S. Tanaka, Phys. Rev. Lett. **73**, 174 (1994).
[36] A. V. Puchkov, T. Timusk, S. Doyle, and A. M. Herman, Phys. Rev. B **51**, 3312 (1995).
[37] D. N. Basov, *et al.*,Science **283**, 4952 (1999).
[38] C. C. Homes, , B. P. Clayman, J. L. Peng, and R. L. Greene, Phys. Rev. B **56**, 5525 (1997).
[39] E. J. Singley, D. N. Basov, K. Kurahashi, T. Uefuji, and K. Yamada, Phys. Rev. B **64**, 224 (2001).
[40] T. Startseva *et al.*, Phys. Rev. B **59**, 7184 (1999).
[41] P. C. Hohenberg, A. Aharony, B. I. Halperin, and E. D. Siggia, Phys. Rev. B **13**, 2986 (1976).
[42] A. Peliasetto and E. Vicari, Physics Reports **368**, 549 (2002).
[43] K.Kim and P.B.Weichman, Phys. Rev. B **43**, 13583 (1991).
[44] P. A. Crowell, F. W. van Keuls, and J. R. Reppy, Phys. Rev. B **55**, 12620 (1997).
[45] Y. Uemura *et al.*, Phys. Rev. Lett. **62**, 2317 (1989).
[46] T. Schneider, Journal of Superconductivity, **17**, 41 (2004).
[47] T. Schneider and D. Di Castro, Phys. Rev. B**69**, 024502 (2004).
[48] Y.J. Uemura *et al.*, Phys. Rev. B **38**, 909 (1988).
[49] S. Komiya, Y. Ando, X. F. Sun, and A. N. Lavrov, Phys. Rev. B **65**, 214535 (2002).
[50] H. Sato,A. Tsukada, M. Naito, and A. Matsuda, Phys. Rev. B **61**, 12447 (2000).
[51] Mun-Seog Kim, John A. Skinta, and T.R. Lemberger, A. Tsukada and M. Naito, cond-mat/0302086.
[52] T. Schneider and H. Keller, Phys. Rev. Lett. **86**, 4899 (2001).
[53] T. Schneider, Phys. Rev. B **67**, 134514 (2003).
[54] K. Conder *et al.*, in *Phase Separation in Cuprate Superconductors*, edited by E. Sigmund and K. A. Muller (Springer, Berlin 1994) p. 210.
[55] F. Raffa, T. Ohno, M. Mali, J. Roos, D. Brinkmann, K. Conder, and M. Eremin, Phys. Rev. Lett. **81**,5912 (1998).
[56] T. Schneider, R. Khasanov, K. Conder, and H. Keller, J. Phys. Condens. Matter **15**, L763 (2003).
[57] R. Khasanov, T. Schneider, J. Karpinski, and H. Keller, cond-mat/0402398.
[58] S. Mo, J. Hove, A. Sudbo, Phys. Rev. B **65**, 104501 (2002).
[59] D. S. Fisher, M. P. A. Fisher and D. A. Huse, Phys. Rev. B **43**, 130 (1991).
[60] I. F. Herbut, Phys. Rev. Lett. **81**, 3916 (1998).
[61] C. Bernhard *et al.*, Phys. Rev. Lett. **86**, 1614 (2001).
[62] C. Niedermayer *et al.*, Phys. Rev. Lett. **71**, 1764 (1993).
[63] T. Schneider, R. Khasanov and H. Keller, to be published.
[64] J. Hofer, K. Conder, T. Sasagawa, Guo-meng Zhao, M. Willemin, H. Keller, and K. Kishio, Phys. Rev. Lett. **84**, 4192 (2000).
[65] R. Khasanov, Studies of the oxygen-isotope effect on the magnetic field penetration depth in cuprate superconductors, Ph.D. Thesis, University of Zürich (2003).
[66] R. Khasanov, A. Shengelaya, K. Conder, E. Morenzoni, I. M. Savic, and H Keller, J. Phys.: Condens. Matter **15**, L17 (2003).
[67] R. Khasanov, A. Shengelaya, E. Morenzoni, M. Angst, K. Conder, I. M. Savic, D. Lampakis, E. Liarokapis, A. Tatsi, and H. Keller, Phys. Rev. B **68**, 220506(R) (2003).
[68] R. Khasanov, D. G. Eshchenko, H. Luetkens, E. Morenzoni, T. Prokscha, A. Suter, N. Garifianov, M. Mali, J. Roos, K. Conder, and H. Keller, Phys. Rev. Lett. **92**, 057602-1 (2004).
[69] R. Khasanov *et al.*, cond-mat/0404428.
[70] R. Khasanov, A. Shengelaya, E. Morenzoni, K. Conder, I.M. Savic, and H. Keller, cond-mat/0404428.
[71] M. B. Maple, C. C. Almasan, C. L. Seaman, S. H. Han, K. Yoshiara, M. Buchgeister, L. M. Paulius, B. W. Lee, D. A. Gajewski, R. F. Jardim, C. R. Fincher Jr., G. B. Blanchet, and R. P. Guertin, J. Superconductivity **7**, 97 (1994).
[72] Y. Dalichaouch, C. L. Seaman, C. C. Almasan, M. C. de Andrade, H. Iwasaki, P. K. Tsai, M. B. Maple, Physica B **171**, 308 (1991).
[73] T. Schneider, cond-mat/0308595.
[74] M. Tinkham, *Introduction to Superconductivity*, McGraw Hill, New York 1975.
[75] S. Gariglio, C. H. Ahn, D. Matthey, and J.-M. Triscone, Phys. Rev. Letters. 88, 067002 (2002).
[76] B. Stojkovic and D. Pines, Phys. Rev. Lett. **76**, 811 (1996); Phys. Rev. B **55**, 8576 (1997).
[77] J. P. Franck, J. Jung, M. A-K. Mohamed, S. Gygax, and G. I. Sproule, Phys. Rev. B 44, 5318 (1991).
[78] G. Sorensen and S. Gygax, Phys. Rev. B 51, 11848 (1995).
[79] W. H. Fietz, R. Quenzel, H. A. Ludwig, K. Grube, S. I. Schlachter, F. W. Hornung, T. Wolf, A. Erb, M. Klaser, and G. Müller-Vogt, Physica C **270**, 258 (1996).
[80] S. Sadewasser, Y. Wang, J. S. Schilling, H. Zheng, A. P. Paulikas, and B. W. Veal, Phys. Rev. B **56**, 14168 (1997).
[81] R. Sieburger and J. S. Schilling, Physica C **173**, 423 (1991).

[82] A.-K. Klehe, C. Looney, J. S. Schilling, H. Takahashi, N. Mori, Y. Shimakawa, Y. Kubo, T. Manako, S. Doyle, and A. M. Hermann, Physica C **257**, 105 (1996).
[83] C. Looney, J. S. Schilling, S. Doyle, and A. M. Hermann, Physica C **289**, 203 (1997).
[84] See J. S. Schilling and S. Klotz, in *Physical Properties of High Temperature Superconductors*, edited by D. M. Ginsberg (World Scientific, Singapore, 1992), Vol. III, p. 59, and references therein.
[85] R. J. Wijngaarden, D. T. Jover, and R. Griessen, Physica B **265**, 128 (1999).
[86] J. S. Schilling, C. Looney, S. Sadewasser, and Y. Wang, Rev. High Pressure Sci. Technol. **7**, 425 (1998).
[87] J. Tang, Y. Okada, Y. Yamada, S. Hori, A. Matsushita, T. Kasaka, and T. Matsumoto, Physica C **282-287**, 1443 (1997).
[88] M. A. Hubbard, M. B. Salamon, and B. W. Veal, Physica C **259**, 309 (1996).
[89] V. Pasler, P. Schweiss, Ch. Meingast, B. Obst, H. Wühl, A. I. Rykov, and S. Tajima, Phys. Rev. Lett. **81**, 1094 (1998).
[90] J. Nyhusa, U. Thisteda, N. Kikugawab, T. Suzukib, and K. Fossheim, Physica C **369**, 273 (2002).
[91] K. Ghiron, M. B. Salamon, B. W. Veal, A. P. Paulikas, and J. W. Downey, Phys. Rev. B **46**, 5837 (1992).
[92] J. W. Loram, K. A. Mirza, J. M. Wade, and J. L. Tallon, Physica C **235-240**, 1735 (1994).
[93] J. W. Loram, K. A. Mirza, J. R. Cooper, and J. L. Tallon, J. Phys. Chem. Solids, **59**, 2091 (1998).
[94] M. R. Trunin, Yu. A. Nefyodov, cond-mat/0306158.